A Role for Phosphoinositide 3-Kinase in the Completion of Macropinocytosis and Phagocytosis by Macrophages

Nobukazu Araki, Melissa T. Johnson, and Joel A. Swanson

Department of Cell Biology, Harvard Medical School, Boston, Massachusetts 02115

Abstract. Phosphoinositide 3-kinase (PI 3-kinase) has been implicated in growth factor signal transduction and vesicular membrane traffic. It is thought to mediate the earliest steps leading from ligation of cell surface receptors to increased cell surface ruffling. We show here that inhibitors of PI 3-kinase inhibit endocytosis in macrophages, not by interfering with the initiation of the process but rather by preventing its completion. Consistent with earlier studies, the inhibitors wortmannin and LY294002 inhibited fluid-phase pinocytosis and Fc receptor–mediated phagocytosis, but they had little effect on the receptor-mediated endocytosis of diI-labeled, acetylated, low density lipoprotein. Large solute probes of endocytosis reported greater inhibition by wortmannin than smaller probes did, indicating that macropinocytosis was affected more than micropinocytosis. Since macropinocytosis and phagocytosis are actin-mediated processes, we expected that their inhibition by wortmannin resulted from deficient signaling

from macrophage colony-stimulating factor (M-CSF) receptors or Fc receptors to the actin cytoskeleton. However, video microscopy showed cell surface ruffling in wortmannin-treated cells, and increased ruffling after addition of M-CSF or phorbol myristate acetate. Quantitative measurements of video data reported slightly diminished ruffling in wortmannin-treated cells. Remarkably, the ruffles that formed in wortmannin-treated macrophages all receded into the cytoplasm without closing into macropinosomes. Similarly, wortmannin and LY294002 did not inhibit the extension of actin-rich pseudopodia along IgG-opsonized sheep erythrocytes, but instead prevented them from closing into phagosomes. These findings indicate that PI 3-kinase is not necessary for receptor-mediated stimulation of pseudopod extension, but rather functions in the closure of macropinosomes and phagosomes into intracellular organelles.

MACROPHAGES are actively endocytic cells, exhibiting measurable fluid-phase pinocytosis, phagocytosis, and receptor-mediated endocytosis of soluble ligands. Receptor-mediated endocytosis occurs principally through clathrin-coated vesicles (12). Fluid-phase pinocytosis includes both macropinocytosis, by pinosomes >0.2-μm diam, and micropinocytosis, by clathrin-coated vesicles and small, uncoated vesicles (32). Macropinosomes originate primarily at the cell margins as actin-rich ruffles that close to form intracellular vesicles. Macrophage colony-stimulating factor (M-CSF)[1] and PMA stimulate

both ruffling and macropinocytosis in macrophages (23, 30). Ruffling and macropinocytosis require a functional actin cytoskeleton, in that both are sensitive to cytochalasins. For growth factor–stimulated pinocytosis, a signal generated by a ligated receptor leads eventually to increased actin polymerization and ruffling. Although ruffling is a prerequisite for macropinosome formation, additional activities may be required to transform a ruffle into a closed intracellular vesicle. To date, no such activities have been identified.

Phagocytosis usually occurs by sequential interactions between macrophage surface receptors and opsonic ligands on surfaces of particles. Pseudopod advance is guided by these tethered ligands, and phagocytosis proceeds as a zipperlike engagement between the macrophage membrane and the particle surface. Current models for phagocytosis are similar to those for growth factor–stimulated ruffling: receptor–ligand interactions signal an increase in actin polymerization near the membrane, and this polymerized actin fills the pseudopod that extends around the particle (15). The pseudopod that forms a phagosome would therefore be analogous to the ruffle that forms a macropino-

Address all correspondence to Joel A. Swanson, Department of Anatomy and Cell Biology, University of Michigan Medical School, Ann Arbor, MI 48109-0616. Tel.: (313) 647-6339. Fax: (313) 763-1166. e-mail: jswan@umich.edu

N. Araki's present address is Department of Anatomy, Ehime University School of Medicine, Ehime 791-02, Japan.

1. *Abbreviations used in this paper:* diI-acLDL, diI-labeled acetylated low density lipoprotein; mBSA, maleylated BSA; M-CSF, macrophage colony-stimulating factor; PI 3-kinase, phosphoinositide 3-kinase; RB, Ringer's buffer.

some. Although it is possible that a zipperlike pseudopod advance would be sufficient to engulf a particle, other activities may be needed to close the phagosome or to sever the small remaining connection to the plasma membrane. Thus, although macropinocytosis and phagocytosis differ in their contents and in the details of signal transduction, they appear mechanistically similar (31).

Phosphoinositide 3-kinase (PI 3-kinase) has been implicated in the regulation of endocytosis, intracellular membrane traffic, and cell growth. Mammalian PI 3-kinase consists of two molecules, a catalytic subunit (p110) and a regulatory subunit (p85). It phosphorylates phosphoinositides at the D3 hydroxyl of inositol, producing phosphatidylinositol 3-phosphate, phosphatidylinositol (3, 4)-bisphosphate, or phosphatidylinositol (3, 4, 5)-trisphosphate (11). The molecules that interact with 3-phosphoinositides to affect cell function are not yet known. Nonetheless, a number of cellular processes require PI 3-kinase activity, including mitogenesis (6), membrane ruffling (18, 36), fluid-phase pinocytosis (3, 8), the respiratory burst (2, 22), and lysosomal enzyme sorting (5, 10, 25). The requirement of PI 3-kinase for growth factor–stimulated ruffling indicates that activation of the enzyme is one of the earliest signals from activated tyrosine kinase receptors.

Two reagents have been useful for studying PI 3-kinase function in cells. Wortmannin irreversibly inhibits the catalytic subunit of mammalian PI 3-kinase, and it does so at low nanomolar concentrations ($IC_{50} = 3$ nM; [1, 33, 38]). It inhibits other enzymes as well, but this inhibition requires higher concentrations of wortmannin (21, 38). LY294002, a quercetin analogue, also specifically inhibits PI 3-kinase. Its inhibitory effects are reversible, and it is specific for PI 3-kinase (35). At concentrations that maximally inhibit PI 3-kinase, LY294002 shows little or no inhibition of other enzymes affected by wortmannin, including phosphatidylinositol 4-kinase (35), myosin light chain kinase (39), or phospholipase A_2 (Vlahos, C.J., personal communication). As a result of their different chemistries of inhibition, similar effects observed using both nanomolar wortmannin and micromolar LY294002 can implicate PI 3-kinase in a cellular activity.

There is presently some confusion about the role of PI 3-kinase in endocytosis. Several studies have indicated that PI 3-kinase is not necessary for receptor-mediated endocytosis of soluble ligands (3, 5, 16, 26, 29) (with one exception, reference 19). In contrast with its negligible effect on receptor-mediated endocytosis, wortmannin greatly inhibits fluid-phase pinocytosis and phagocytosis (3, 8, 19, 22) (with two reported exceptions, references 2, 28). It is not clear why the different kinds of endocytosis show such different responses to inhibitors of PI 3-kinase. One possible explanation is that PI 3-kinase has a more significant role in the intracellular membrane traffic that follows internalization (16, 29), and that inhibition of this postendocytic traffic affects rates of fluid-phase endocytosis more than rates of receptor-mediated endocytosis (27).

Another possible explanation for the different effects of wortmannin on receptor-mediated endocytosis and pinocytosis or phagocytosis is that PI 3-kinase selectively inhibits actin-dependent endocytosis. Since PI 3-kinase is necessary for the ruffling that follows binding of PDGF (36), insulin, or insulin-like growth factor-1 (18) to their

receptors, it may be that wortmannin inhibits pinocytosis and phagocytosis secondarily, by inhibiting the signaling necessary for pseudopod formation. Other components of actin-mediated endocytosis could be regulated by PI 3-kinase as well.

As no data are presently available about the role of PI 3-kinase in fluid-phase pinocytosis and receptor-mediated endocytosis in macrophages, and the data on phagocytosis are conflicting, the enzyme's contribution to each of the three major categories of endocytosis remains unclear. Here we examine the role of PI 3-kinase in endocytosis by characterizing the effects of wortmannin and LY294002 in bone marrow–derived macrophages. Our results indicate that PI 3-kinase is not necessary for receptor-mediated endocytosis of a soluble ligand, nor does it participate in the signal transduction that initiates ruffling or phagocytosis. Rather, it is necessary for completion of actin-dependent endocytosis.

Materials and Methods

Reagents

Wortmannin was purchased from Sigma Chemical Co. (St. Louis, MO) and was reconstituted to 10 mM in DMSO. LY294002, generously provided by Dr. Chris Vlahos (Lilly Research Laboratories, Indianapolis, IN), was reconstituted to 50 mM in DMSO. Both were stored at $-80°C$ and diluted in media just before use. Lysine-fixable and nonfixable fluorescein-dextrans, average mol wt 3,000 (FDx3), 10,000 (FDx10), 70,000 (FDx70), and Texas red dextrans, average mol wt 10,000 (TRDx10) and 70,000 (TRDx70); diI-labeled, acetylated low density lipoprotein (diI-acLDL); rhodamine-phalloidin; and NBD-phallicidin were obtained from Molecular Probes, Inc. (Eugene, OR). Lucifer yellow was purchased from Aldrich Chemical Co. (Milwaukee, WI). Fluorescein dextran, average mol wt 150,000, was purchased from Sigma Chemical Co. and was further size-fractionated by gel permeation chromatography (4). Recombinant human M-CSF was donated by Genetics Institute (Cambridge, MA). Sheep blood alsevers and rabbit anti–sheep erythrocyte IgG were obtained from Organon Teknika–Cappel (Durham, NC). Rabbit anti–cathepsin D serum was a gift from Dr. Sadaki Yokota (Yamanashi Medical School, Japan). Anti-tubulin mAb (E7) was obtained from the Developmental Studies Hybridoma Bank maintained by the Department of Pharmacology and Molecular Sciences, Johns Hopkins University, and the Department of Biological Sciences, University of Iowa. All other reagents were purchased from Sigma Chemical Co., unless otherwise indicated.

Cell Culture

Murine bone marrow–derived macrophages were obtained as previously described (30). Bone marrow exudate was obtained from femurs of female C3H HeJ mice (The Jackson Laboratory, Bar Harbor, ME). The exudate was cultured in medium that promotes growth and differentiation of macrophages (bone marrow culture medium: 30% L-cell–conditioned medium, a source of M-CSF, 20% heat inactivated in FBS DME). After 6 or 7 d of culture, macrophages were harvested from dishes and plated onto 12- or 25-mm circular coverslips or 24-well culture dishes. Cultures were then incubated overnight in medium lacking M-CSF (DME-10F: DME with 10% heat-inactivated FBS). All experiments were performed the day after plating.

Cell Labeling with Endocytic Markers

Nonfixable FDx3, FDx10, FDx70, FDx150, and lucifer yellow were used to measure fluid-phase pinocytosis. For combined immunofluorescence and phalloidin staining, lysine-fixable FDx3, FDx10, FDx70, TRDx10, and TRDx70 were used. The cells were incubated for various intervals in Ringer's buffer (RB: 155 mM NaCl, 5 mM KCl, 1 mM MgCl$_2$, 2 mM Na$_2$HPO$_4$, 10 mM glucose, 10 mM Hepes, pH 7.2, 0.5 mg/ml BSA) containing one or two fluid-phase markers. For pulse-chase experiments, the cells were incubated in RB containing a fluorescent probe for 5 or 30 min at 37°C, washed, and incubated in RB without marker for different times.

To measure receptor-mediated endocytosis, diI-acLDL was prepared and used as previously described (24). Macrophages were incubated in medium containing 5 μg/ml diI-acLDL at 37°C for 5 or 30 min to allow endocytosis. For acLDL-binding studies, the cells were exposed to diI-acLDL at 4°C for 30 min. Nonspecific endocytosis and binding of diI-acLDL were measured in the presence of 250 μg/ml maleylated BSA (mBSA; 13, 17). Reported values were corrected by subtracting the values for nonspecific labeling.

Quantitation of fluorophores was performed as described previously (4, 30). After incubation to allow either fluid-phase pinocytosis or receptor-mediated endocytosis of diI-acLDL, dishes were drained and rinsed twice in 1 liter PBS plus 1 mg/ml BSA and then once in 1 liter PBS, each at 4°C for 5 min. Dishes were drained and cells were lysed in 0.5 ml lysis buffer consisting of 0.1% Triton X-100 and 50 mM Tris, pH 8.5. The fluorescence of lysates was measured in a spectrofluorometer (500 C; SLM-AMINCO, Urbana, IL). Fluorescein was measured at excitation 495 nm, and emission 514 nm. Lucifer yellow was measured at excitation 430 nm and emission 580 nm. These wavelengths allowed selective measurement of each fluorophore when the cells were labeled with both fluorescein and lucifer yellow (4). DiI-acLDL was measured at excitation 520 nm and emission 567 nm. Protein concentration in lysates was measured by the bicinchoninic acid assay (BCA; Pierce Chemical Co., Rockford, IL).

For phagocytosis measurements, sheep erythrocytes were washed in PBS, opsonized with anti–sheep erythrocyte IgG (Organon Teknika–Cappel) at 1:50 dilution in PBS for 1 h at 37°C, and resuspended in PBS at 10⁹ erythrocytes per ml. 10 μl of opsonized erythrocyte suspension was added to each well containing macrophages on 12-mm coverslips. Macrophages were incubated for 30 min at 37°C to allow phagocytosis. To identify internalized sheep erythrocytes, extracellular erythrocytes bound to the surface of macrophages were ruptured by dipping coverslips into distilled water for 30 s (37). Cells were then fixed, and the number of erythrocytes per 100 macrophages was counted as the phagocytic index.

To visualize phagocytosis by fluorescence confocal microscopy, sheep erythrocytes were labeled covalently with NHS-biotin, and then opsonized with IgG and surface labeled with fluorescein-streptavidin. 15 μl of NHS-biotin (50 mg/ml in dimethyl formamide) was added to 5 × 10⁸ washed erythrocytes in 1 ml 150 mM carbonate buffer. After 20 min on ice, cells were washed three times in PBS, and then were opsonized with rabbit anti–sheep erythrocyte IgG as described above. Macrophages on coverslips were preincubated 30 min in 0.5 ml RB +/− 100 nM wortmannin, and then were given 5 × 10⁶ (10 μl) biotinylated, opsonized erythrocytes plus 100 μl of fluorescein-streptavidin (40 μg/ml in RB/BSA). After 15 min to allow phagocytosis, cells were washed free of unbound erythrocytes, fixed for 30 min at 37°C (fixative = 3.8% formaldehyde, 0.25 M sucrose, 1 mM EGTA, 0.5 mM EDTA, 20 mM Hepes, pH 7.4), stained with rhodamine-phalloidin (5 min at 5 U/ml in PBS + 0.25% Triton X-100), and then mounted in glycerol with phenylenediamine for viewing by fluorescence confocal microscopy.

Drug Treatments

Effects of wortmannin and LY294002 were assessed after a 30-min preincubation at the concentrations indicated, followed by incubation with endocytic probes in the presence of the drugs. Control cells were treated with 0.1% DMSO, the final concentration of DMSO in preparations treated with wortmannin and LY294002. PMA at 60 ng/ml was applied 30 min before the incubation with fluorophores and at the same time that probes were added. M-CSF at 2,000 U/ml was added at the same time as the endocytic probes.

Fluorescence Microscopy

To observe fluorescent probes internalized by fluid-phase pinocytosis and receptor-mediated endocytosis, macrophages on 12-mm, No. 1 coverslips were incubated with fluorophores as described above, washed, and then fixed with 4% paraformaldehyde in 40 mM Hepes buffer, pH 7.4, containing 6.5% sucrose for 1 h at 37°C. After rinsing again with PBS, the coverslips were mounted on glass slides. After fixation, some specimens were further rinsed with 0.25% NH₄Cl in PBS, permeabilized with 0.25% Triton X-100 in PBS, and processed for immunofluorescence, or for F-actin localization using rhodamine-phalloidin or NBD-phallicidin. Rabbit anti–cathepsin D serum was diluted 1:500, and mouse monoclonal E7 antibody that recognizes tubulin was diluted 1:5 in PBS containing both 0.25% Triton X-100 and 2% heat-inactivated goat serum. As secondary antibodies, fluorescein or Texas red–labeled antibodies against rabbit IgG or mouse

IgG (Vector Laboratories, Inc., Burlingame, CA) were used at 1:250 dilution. Rhodamine-phalloidin was used at 6 U/ml in PBS containing 0.25% Triton X-100. Specimens were observed in an epifluorescence microscope (Carl Zeiss, Inc., Thornwood, NY) and photographed using T-Max 400 film (Eastman Kodak Co., Rochester, NY).

Confocal images were collected with a laser scanning confocal fluorescence microscope (Axiovert 135 TV; Carl Zeiss, Inc.), with a ×63, NA 1.4 objective lens. Settings allowed simultaneous colocalization of fluorescein-labeled erythrocytes and rhodamine-phalloidin–stained macrophages (laser line = 488, 568; emission filters = LP590, BP515-540). The rhodamine-phalloidin did not label the erythrocytes.

Video Microscopy

Macrophages plated onto 25-mm-diam coverslips (2 × 10⁵ per coverslip) were assembled into Leiden chambers (Medical Systems Corp., Greenvale, NY). The chambers were filled with 1.0 ml RB, sealed with silicon oil (Fisher Scientific, Fair Lawn, NJ), and placed in a temperature-controlled stage heater set at 37°C on an inverted microscope (IM-35; Carl Zeiss, Inc.). Cells were observed using a ×100 lens, N.A. 1.32, with phase-contrast optics. To add wortmannin, 0.5 ml RB was removed from the chamber and replaced with RB containing 200 nM wortmannin. PMA and M-CSF were similarly applied as 2× stocks in RB. Cytochalasin D was added to cells in RB by adding a concentrated stock (5 mM in DMSO) to a final concentration of 10 μM. Chambers were left 15–30 min after addition of drugs before images were recorded. Images were collected by a video camera (NC-66X; Dage-MTI Inc., Wabash, MI) mounted on the microscope. Time-lapse video recordings were collected using MetaMorph 2.0 image analysis software (Universal Imaging Co., West Chester, PA) and stored in a file server or an optical disc recorder (Panasonic, Secaucus, NJ).

Quantitative Analysis of Ruffling

To quantify ruffling, phase-contrast images of macrophages were collected as a time-lapse series, digitizing one frame every 5 s for 2 min to assemble a stack of 25 images. In movies made from these stacks, the movements of ruffles were evident as phase-dense bands that grew in length and migrated centripetally along the upper surface of the cells. We quantified this activity by measuring the fraction of the pixels in an image of the cell whose phase density changed by >20 U of gray value (gray scale of 0–255) in a 15-s interval. Independent measurements determined that 15-s intervals maximized signals from ruffles and minimized signals from organelle movements (data not shown). From the stack of 25 images, a macrophage in frame 15 was traced manually to obtain a binary mask of its profile. Then frame 12 was subtracted digitally from frame 15, and a value of 100 was added to all pixels. If there were no cellular motion in the 15-s interval between frames (or if a frame had been subtracted from itself), then the resulting image would be a uniform gray field, and a histogram of the pixels within the cell profile would show all pixels with a value of 100. Histograms of moving cells were Gaussian curves centered at a gray value of 100. To quantify this movement, pixels within the cell profile (defined by the binary) with gray values of 0–80 or 120–255 were counted and divided by the total number of pixels in the cell profile.
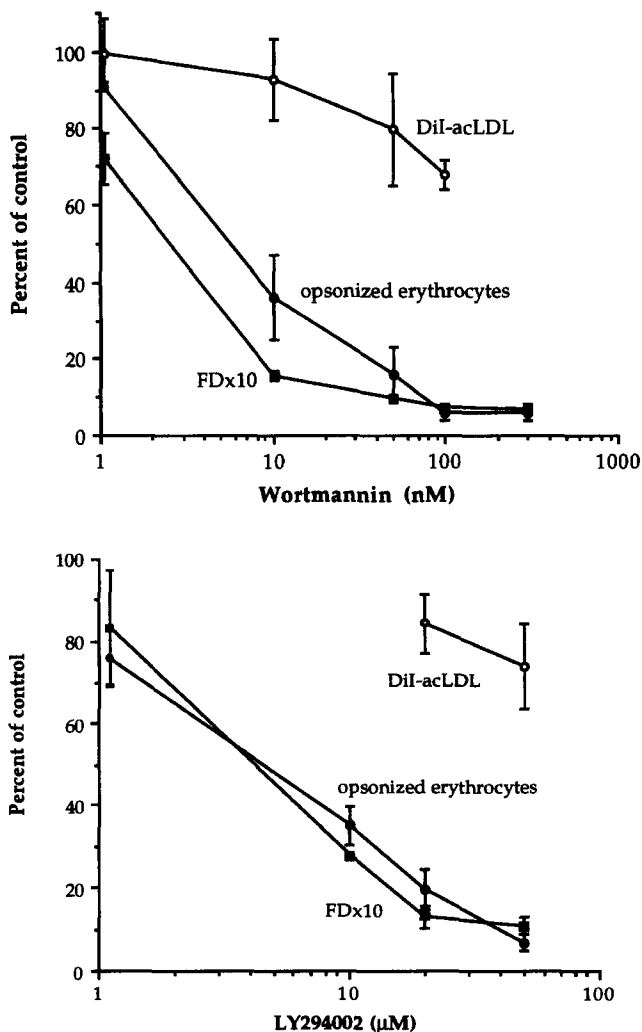
Scanning EM

Macrophages on coverslips were fixed with 2% glutaraldehyde in 0.1 M cacodylate buffer, pH 7.4, containing 6.8% sucrose, for 1 h at room temperature. Coverslips were then rinsed in buffer, postfixed with 1% osmium tetroxide in 0.1 M cacodylate buffer for 1 h at 4°C, and treated with 1% tannic acid in distilled water for 30 min, and then 1% osmium tetroxide for 30 min at 4°C. After dehydration in a graded ethanol series, they were immersed in t-butyl alcohol overnight, frozen at −20°C, and dried in a t-butyl alcohol freeze drier (VFD-21; Vacuum Device Inc., Ibaraki, Japan). Specimens were coated with platinum using an ion-coater and observed with a scanning electron microscope (S-800; Hitachi Ltd., Tokyo, Japan).

Results

Effects of Wortmannin and LY294002 on Pinocytosis

The PI 3-kinase inhibitors wortmannin and LY294002 inhibited fluid-phase pinocytosis of FDx10, with half-maxi-
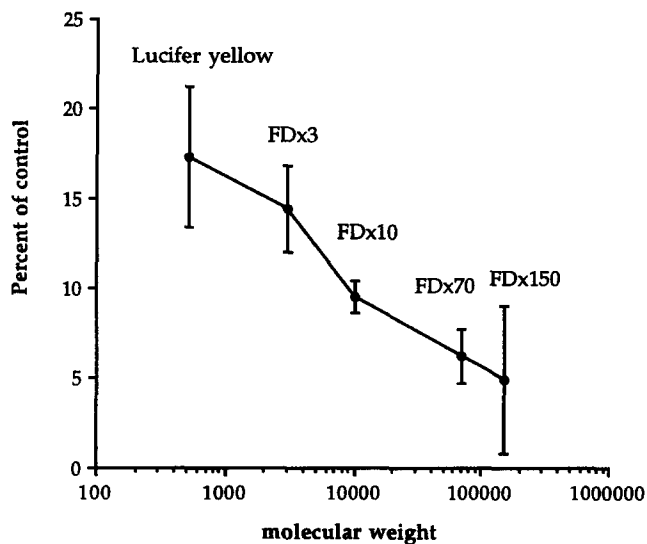
probably because larger molecules have limited access to small endocytic vesicles (4). This size-selective influx is less evident after stimulation of macropinocytosis, when average pinosome dimensions are larger (30; data not shown). When the effects of wortmannin on pinocytosis were measured using lucifer yellow (mol wt 457) instead of FDx10 (average mol wt 10,000), the dose–response curve was similar to that of Fig. 1, but the extent of inhibition was less pronounced (data not shown). We postulated that the different inhibition measured using these two probes reflected a decrease in the average size of pinosomes made by wortmannin-treated cells. Accordingly, if larger probes preferentially label macropinosomes, and macropinocytosis is selectively inhibited by wortmannin, then the largest probe of pinocytosis should report the greatest inhibition by the drug. To test this, we measured the effects of 100 nM wortmannin using lucifer yellow and different sizes of fluorescein dextran: FDx3, FDx10, FDx70, and FDx150. Consistent with a selective inhibition of macropinocytosis by wortmannin, larger molecules showed a greater inhibition than small molecules did (Fig. 2).

Fluorescence microscopy supported this interpretation. Controls pulsed 5 min with small probes such as lucifer yellow or FDx3 in the presence of M-CSF showed fluorescent labeling of both macropinosomes and small pinosomes (Fig. 3, a and b). Similar exposure to FDx150 labeled only macropinosomes (Fig. 3, c and d). These images indicated that small endocytic vesicles labeled better with small probes than with large probes. Wortmannin-treated cells contained no labeled macropinosomes. Instead, lucifer yellow and FDx3 labeled only small vesicles (Fig. 3, e and f), and FDx150 did not label anything (Fig. 3, g and h). Thus, the different sized probes allowed us to discriminate between large and small pinosomes and revealed that wort-

Figure 1. Dose-dependent inhibitory effects of wortmannin (*upper graph*) and LY294002 (*lower graph*) on fluid-phase pinocytosis of FDx10, receptor-mediated endocytosis of diI-acLDL, and phagocytosis of opsonized sheep erythrocytes. Macrophages were preincubated 30 min with wortmannin or LY294002 at the concentrations indicated. Cells were further incubated with FDx10 (0.5 mg/ml), diI-acLDL, or IgG-opsonized erythrocytes for 30 min at 37°C in the presence or absence of the drugs. Quantitation of pinocytosis, phagocytosis, and receptor-mediated endocytosis of diI-acLDL is described in the Material and Methods. All values are expressed as percentage of control. For FDx10 and diI-acLDL, each point represents the mean ± SD of triplicate determinations; essentially the same results were obtained in two additional experiments. Phagocytosis data represent pooled results from two independent experiments.

mal inhibition by wortmannin at 3 nM, and by LY294002 at 3 μM (Fig. 1). These dose–response curves were comparable to the measured effects of these inhibitors on PI 3-kinase (35, 38). Since fluid-phase pinocytosis was maximally inhibited by 100 nM wortmannin and 50 μM LY294002, these concentrations were used in further experiments.

Using different sized fluorescent probes, we determined that wortmannin selectively inhibited macropinocytosis. Earlier studies had indicated that large probes of pinocytosis enter macrophages less efficiently than small probes,

Figure 2. Inhibitory effect of wortmannin on fluid-phase pinocytosis of different sized molecules. Cells were preincubated with 100 nM wortmannin or 0.1% DMSO only (control) in RB for 30 min, and then incubated with probes (0.5 mg/ml) in the presence or absence of wortmannin for 30 min at 37°C. The fluorescence of lysates was measured. Values are expressed as percentage of control (no wortmannin) for each probe (e.g., FDx10 accumulated in wortmannin/FDx10 accumulated without wortmannin × 100).
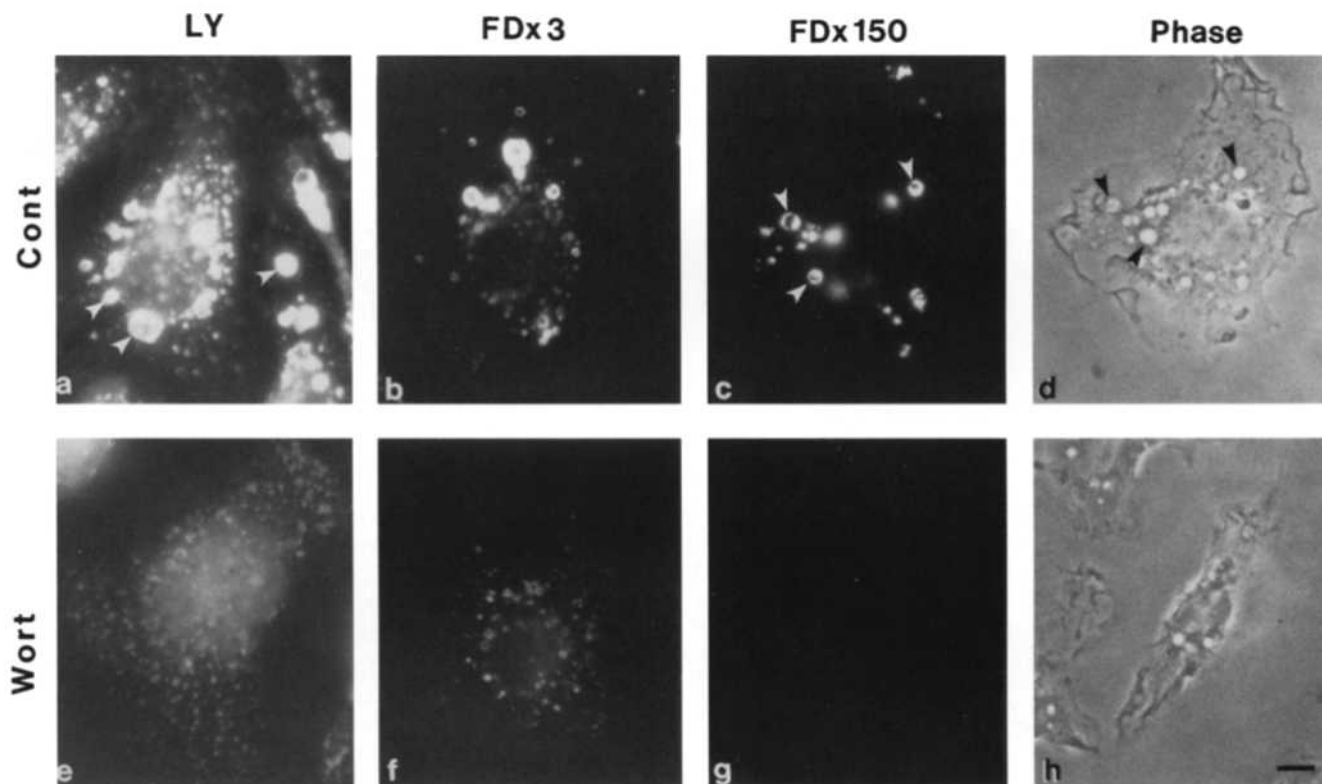
Figure 3. Wortmannin selectively inhibited macropinocytosis. Fluorescence micrographs show control and wortmannin-treated cells given either lucifer yellow (*a* and *e*), FDx3 (*b* and *f*), or FDx150 (*c, d, g,* and *h*) at 0.5 mg/ml for 5 min in the presence of M-CSF. In control cells, lucifer yellow and FDx3 label both macropinosomes (*arrowheads*) and micropinosomes (*a* and *b*), and FDx150 predominantly labels macropinosomes (*c, arrowheads*), which are visible in the corresponding phase-contrast image (*d*). In wortmannin-treated cells, lucifer yellow and FDx3 label micropinosomes, but macropinosomes are not evident (*e* and *f*). FDx150 labeling was undetectable in wortmannin-treated cells. Similar findings were obtained when the concentrations of FDx3 and FDx150 were normalized for fluorescein fluorescence. Bars, 10 μm.
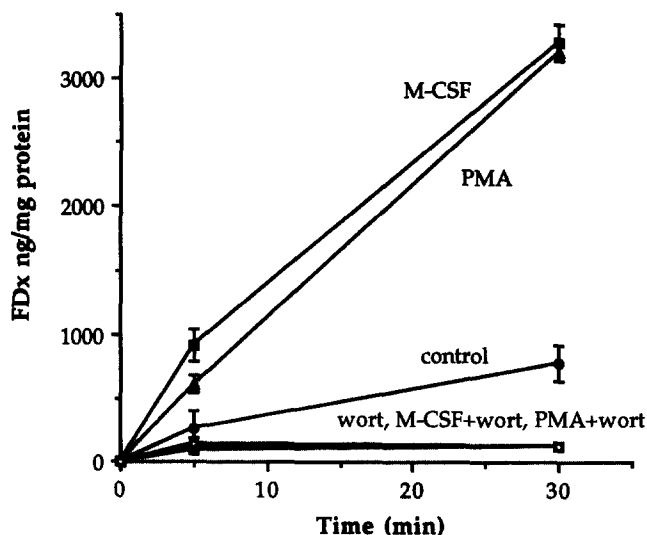
mannin inhibited macropinocytosis more than micropinocytosis.

M-CSF and PMA stimulate macropinocytosis in macrophages (23, 30). M-CSF signals via cell surface receptors and PMA activates protein kinase C. To ask where PI 3-kinase functions relative to M-CSF receptors and protein kinase C, we measured M-CSF– and PMA-stimulated macropinocytosis in wortmannin-treated cells. Whereas both M-CSF and PMA increased the intracellular accumulation of FDx150 about threefold in control cells, neither PMA nor M-CSF showed any stimulatory effects in wortmannin-treated cells (Fig. 4). Inhibition by wortmannin of PMA- or M-CSF–stimulated pinocytosis was apparent even at 5 min, indicating that wortmannin inhibited influx rather than recycling. Direct measurements of efflux showed no significant effects of wortmannin (data not shown).

Despite its dramatic effects on pinocytosis, wortmannin did not disrupt lysosome morphology. Macrophage tubular lysosomes could be labeled in control preparations by a 30-min pulse with fixable FDx10, followed by a 30-min chase in unlabeled medium (Fig. 5, *a* and *b*). These lysosomes contained cathepsin D. In wortmannin-treated cells pulsed and chased similarly with FDx10, cathepsin D–positive tubular lysosomes were still evident, but they were not labeled with FDx10 (Fig. 5, *c* and *d*). Consistent with the size-selective endocytosis noted above, we found that

the tubular lysosomal compartment could be labeled by endocytosis of lucifer yellow in wortmannin; although the extent of labeling was much less than that in controls. Wortmannin treatment prevented lysosomal labeling by endocytosis of FDx150 (Araki, N.; data not shown). Macrophages treated with 20 or 50 μM LY294002 and pulse labeled with FDx10 showed similarly low labeling of lysosomes with FDx10 (data not shown). When lysosomes were prelabeled by endocytosis of 50 μg/ml Texas red ovalbumin before wortmannin treatment, Texas red labeled a compartment that remained tubular after addition of wortmannin (data not shown). Consistent with reports by Brown et al. (5) and Davidson (10), we observed some vacuolation, presumably of prelysosomal compartments, in some macrophages 90 min after addition of wortmannin. These vacuoles were not macropinosomes, and they were scarce in macrophages treated with 100 nM wortmannin.

Wortmannin also did not measurably disrupt the organization of actin filaments or microtubules. After fixing and staining with rhodamine-phalloidin, no clear difference in the general distribution of actin filaments was observed between control and wortmannin-treated cells (see below). Moreover, immunofluorescent localization of tubulin revealed that the generally radial organization of microtubules was unaltered by wortmannin (data not shown).

Figure 4. Wortmannin inhibited M-CSF– and PMA-stimulated pinocytosis of FDx150. Macrophages were pretreated with 0.1% DMSO only (control) or 100 nM wortmannin for 30 min before incubation with FDx150. M-CSF (2,000 U/ml) was added to the medium at the same time as FDx150. PMA (60 ng/ml) was added 30 min before addition of endocytic probes. Cells were incubated with 0.5 mg/ml FDx150 at 37°C, for the times indicated, in the presence of wortmannin, PMA, and M-CSF, as indicated. Fluorescence of lysates was measured; values represent mean and SD of triplicate determinations. Similar results were obtained in two additional experiments.

Effects of Wortmannin and LY294002 on Receptor-mediated Endocytosis

Consistent with a differential role for PI 3-kinase in macro- and micropinocytosis, concentrations of wortmannin and LY294002 inhibitory for pinocytosis inhibited only slightly the receptor-mediated endocytosis of diI-acLDL (Fig. 1). Fluorescence microscopy of the cells pulse labeled 5 or 30 min with diI-acLDL showed that probe was internalized in small vesicles, presumably clathrin-coated vesicles (12) (Fig. 6 a); macrophages pretreated with 100 nM wortmannin looked much the same (Fig. 6 b). To confirm that the observed uptake of diI-acLDL was receptor mediated, labeling and endocytosis of diI-acLDL were measured in the presence and absence of excess mBSA, which competitively binds the scavenger receptor (13, 17). mBSA reduced the fluorometric signal >90% and the fluorescence microscopic labeling to undetectable levels (Fig. 6 c).

Wortmannin and LY294002 showed little effect on either the 5-min accumulation rate, an estimate of influx, or the binding of diI-acLDL at 4°C, a measure of surface-binding activity (Table I). We therefore conclude that PI 3-kinase was not necessary for the receptor-mediated endocytosis of acLDL.

Effect of Wortmannin on Ruffling

PI 3-kinase was also apparently unnecessary for ruffling. When viewed by time-lapse video microscopy, control macrophages ruffled at their dorsal surface and marginal edges. Circular ruffles generated at the cell margin often

closed into phase-bright macropinosomes. Ruffling and macropinocytosis increased after addition of M-CSF (Fig. 7 a). Like controls, wortmannin-treated cells ruffled at the dorsal surface. Ruffling at the cell margins seemed slightly reduced. Addition of M-CSF increased ruffling in wortmannin-treated cells, and circular ruffles were seen frequently (Fig. 7 b). Active ruffling was also observed in macrophages treated with wortmannin plus PMA (data not shown). Scanning EM of macrophages in wortmannin showed extensive ruffling of the cell surface (Fig. 8 b).

We developed a quantitative assay for the movements of ruffles in macrophages. The ruffling index, described in Materials and Methods, reported the fraction of pixels in the macrophage image whose intensity gray values changed >20 U (scale of 0–255) in a 15-s interval. Control macrophages (RB) showed a moderate level of ruffling in time-lapse movies, which gave ruffling index values of 0.18–0.30 (Fig. 9). Pretreatment of cells with cytochalasin D completely inhibited the ruffling in video sequences and reduced the index values to 0.10. This reduction was statistically significant ($P < .001$; two-tailed t test). Macrophages incubated with wortmannin showed only a slight reduction in the ruffling index, which was still considerably greater than that measured in cytochalasin D–treated macrophages, and not statistically different from controls ($P > .05$).

Remarkably, the ruffles formed in wortmannin-treated cells failed to close into macropinosomes. Instead, they simply receded into the cytoplasm (Fig 7 b). Similar results were obtained with PMA: wortmannin-treated cells ruffled but made no macropinosomes. These results indicate that wortmannin inhibited macropinocytosis not by inhibiting the signaling mechanisms leading from M-CSF receptors or from protein kinase C to the generation of cell surface ruffles, but rather by inhibiting the subordinate process of ruffle closure into macropinosomes.

Effects of Wortmannin and LY294002 on Phagocytosis

To examine the role of PI 3-kinase in phagocytosis, macrophages were fed IgG-opsonized erythrocytes in the presence of wortmannin or LY294002. After 30 min, extracellular erythrocytes were lysed by a 30-s exposure to distilled water, a treatment that leaves macrophages and intracellular erythrocytes intact (9, 37). The phagocytic index was then scored as the number of intracellular erythrocytes per 100 macrophages. By this measure, wortmannin and LY294002 inhibited phagocytosis with a dose dependency similar to that observed for pinocytosis (Fig. 1, a and b).

Curiously, however, before osmotic lysis of extracellular erythrocytes, the wortmannin-treated cells appeared to have partially enclosed the erythrocytes. By scanning EM, many wortmannin-treated macrophages contained erythrocytes in cuplike pseudopodia (Fig. 8, d and e), whereas control preparations indicated complete phagocytosis (Fig. 8 c). Rhodamine-phalloidin staining of F-actin in macrophages fed fluorescently labeled erythrocytes showed by fluorescence confocal microscopy that macrophages in wortmannin or LY294002 extended pseudopodia partway around erythrocytes (Fig. 10). In control macrophages, only a few erythrocytes appeared in phagocytic cups stained with rhodamine-phalloidin, as most had been

FDx10   Cathepsin D
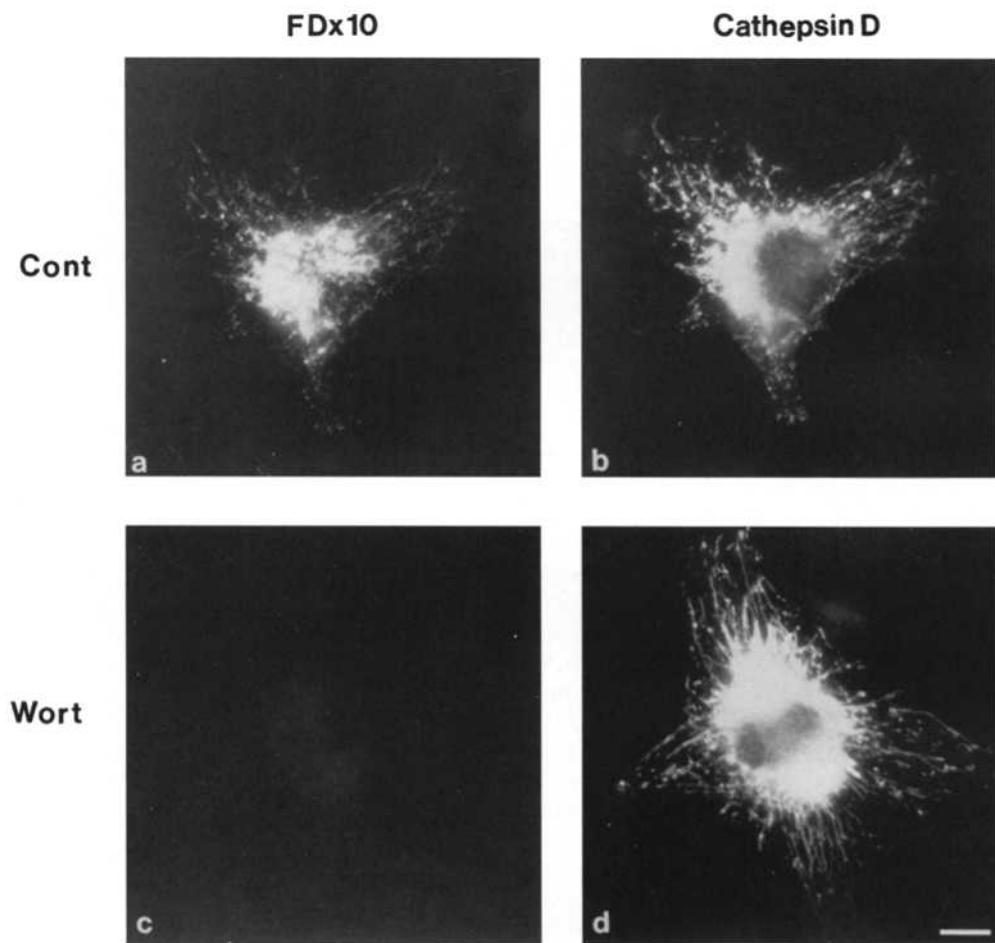
Figure 5. Wortmannin in-hibited pinocytosis without altering lysosome morphology. Macrophages were treated with 0.1% DMSO (control; *a* and *b*) or 100 nM wortmannin (*c* and *d*) for 30 min, and then were incubated with 0.5 mg/ml lysine-fixable FDx10 for 30 min, followed by chase in probe-free medium in the presence or absence of wortmannin. After fixation, cells were stained to localize cathepsin D. (*a* and *c*) FDx10 images; (*b* and *d*) cathepsin D distribution in corresponding cells. Bar, 10 μm.

completely internalized into phagosomes that had then lost their associated F-actin. Wortmannin-treated cells displayed more F-actin–rich phagocytic cups than control cells, presumably because they were unable to complete phagosome closure and subsequent denuding of actin from the phagosome (Figs. 8 and 10). Thus, wortmannin and LY294002 did not interfere with binding of opsonized erythrocytes to Fc-receptors, or with pseudopod extension over the erythrocyte surface. Rather, they apparently inhibited the closure of pseudopodia into phagosomes.

Discussion

The present study indicated two novel conclusions. First, PI 3-kinase was necessary for macropinocytosis and phagocytosis, but not for micropinocytosis or receptor-mediated stimulation of pseudopod extension. Second, PI 3-kinase contributed to a late step in the formation of macropinosomes and phagosomes, probably the closure of pseudopodia to form intracellular vesicles. This late step is subordinate to the mechanism that signals pseudopod extension, but is nonetheless essential.

Fluid-phase pinocytosis and phagocytosis were inhibited by wortmannin with an IC_{50} of 3 nM and maximal inhibition at 100 nM. LY294002, another specific PI 3-kinase inhibitor that is structurally unrelated to wortmannin, also showed dose-dependent inhibitory effects. Since LY294002

is specific for PI 3-kinase and is not known to inhibit other kinases affected by wortmannin, we infer that the common inhibitory effects observed using wortmannin and LY294002 reflect inactivation of PI 3-kinase.

PI 3-Kinase Affects Macropinocytosis More Than Micropinocytosis

An earlier study suggested that different sized probes of endocytosis can be used to gauge the dimensions of endocytic compartments or their communicating vesicles (4). Accordingly, smaller vesicles internalize small molecules such as lucifer yellow more efficiently than large molecules like FDx150. In the present study, the apparent inhibition of pinocytosis by wortmannin increased with the molecular size of the probe used to measure it, consistent with the interpretation that wortmannin inhibited the formation of large vesicles more than the formation of small vesicles. This was supported by fluorescence microscopy. FDx150 labeled predominantly macropinosomes in control cells, and wortmannin treatment inhibited FDx150 endocytosis completely. FDx3 or lucifer yellow could label both macro- and micropinosomes of controls, and after wortmannin treatment, only small vesicles were labeled. Therefore, the decreased uptake of fluid-phase probes by the inhibitors reflected a selective effect on macropinocytosis.
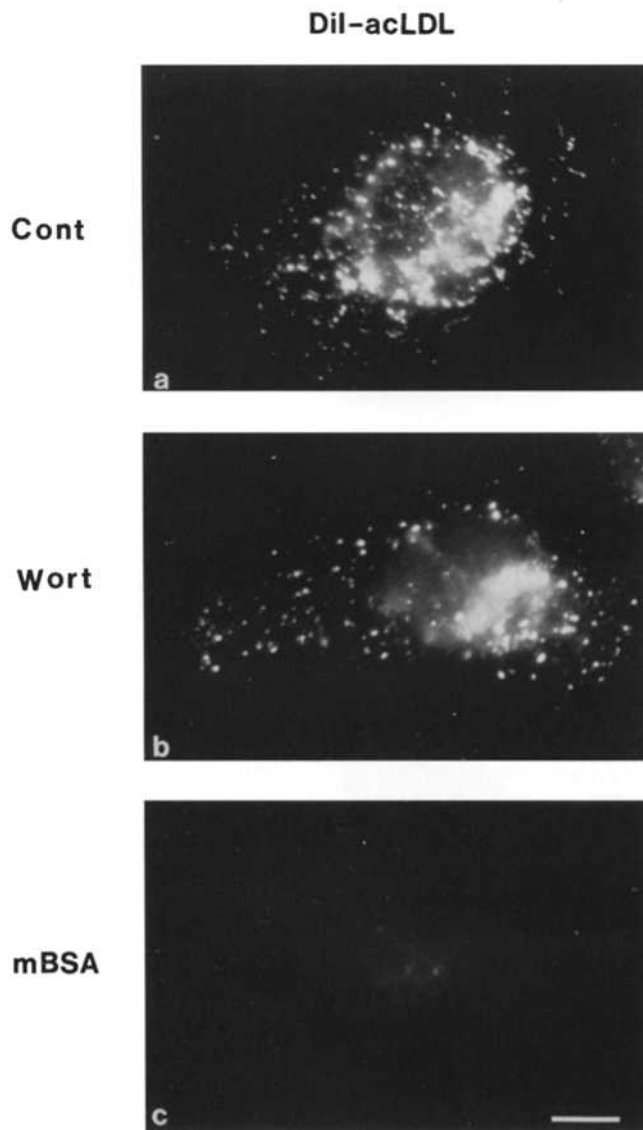
DiI–acLDL

Figure 6. Effects of wortmannin on receptor-mediated endocytosis of diI-acLDL. Macrophages on coverslips were preincubated with 0.1% DMSO (control; *a*) or 100 nM wortmannin (*b* and *c*), then further incubated with 5 µg/ml diI-acLDL in the presence or absence of the drug for 30 min. DiI-acLDL labeled small vesicles in both control and wortmannin-treated cells (*a* and *b*). Coincubation with 250 µg/ml mBSA largely abolished cellular labeling with diI-acLDL (*c*), indicating that the fluorescence in *a* and *b* represents receptor-mediated endocytosis of diI-acLDL. Bar, 10 µm.

Micropinocytosis occurs by at least two kinds of endocytic vesicle: clathrin-coated vesicles, which mediate most receptor-mediated endocytosis, and small, uncoated vesicles. Since receptor-mediated endocytosis of diI-acLDL, which probably occurs via clathrin-coated vesicles (12), was not much affected by wortmannin, we infer that fluid-phase pinocytosis via clathrin-coated vesicles was not greatly affected either. Judging from lucifer yellow fluorescence, it appeared that pinocytosis via small vesicles was slightly decreased by wortmannin, but we could not distinguish the contributions of coated and uncoated vesicles to micropinocytosis.

In addition to the one soluble ligand of receptor-mediated endocytosis described here, others measuring receptor-mediated endocytosis have observed similar insensitivity to wortmannin (3, 5, 26). Deletion of the kinase insert region of the colony-stimulating factor receptor (7) and mutations in the PI 3-kinase–binding domain of the PDGF receptor (16) did not affect receptor internalization, although receptor degradation was affected. However, a role for PI 3-kinase in receptor-mediated endocytosis should not be excluded. Wortmannin reduced transferrin receptor internalization in one study (19), and increased it in another (29). Other studies have indicated relationships between PI 3-kinase and components of clathrin-coated vesicles. The p85 subunit of PI 3-kinase contains an Src homology 3 (SH3) domain that can bind to dynamin, a protein implicated in clathrin-mediated endocytosis (14, 34). Therefore, it remains possible that PI 3-kinase participates in some kinds of receptor-mediated endocytosis.

PI 3-Kinase in the Signaling to Pseudopod Formation

Vigorous ruffling by macrophages in wortmannin was unexpected. Despite their role in macropinocytosis in macrophages (23), distributions of neither microtubules nor F-actin were significantly perturbed by wortmannin. Other studies have demonstrated a role for PI 3-kinase in growth factor–induced ruffling (18, 36). Our different results may be explained by differences in the underlying receptor signaling mechanisms. Some receptors, like those for PDGF, insulin, and insulin-like growth factor-1, use PI 3-kinase in the signal transduction for ruffling (18, 36), whereas others, including the M-CSF receptor, the Fc receptor, and perhaps also the EGF receptor (18), do not. The p85 subunit of PI 3-kinase binds phosphotyrosine residues of several tyrosine kinase receptors after agonist binds receptor, and there is evidence that PI 3-kinase is involved in the early signal transduction from ligated receptors (20). Fc receptors do not contain tyrosine kinase domains, but they asso-

Table I. Quantitative Analysis of the Effects of Wortmannin and LY294002 on Receptor-mediated Binding and Uptake of diI-labeled acLDL

	Control	Wortmannin	LY294002
Binding at 4°C, 30 min	1,065 ± 15.8 (100%)	1,097 ± 142.8 (103%)	954 ± 70.9 (90%)
Uptake at 37°C, 5 min	2,122 ± 153.6 (100%)	1,782 ± 345.8 (73%)	2,054 ± 65.6 (77%)

Macrophages were pretreated with 0.1% DMSO (control), 100 nM wortmannin, or 50 µM LY294002 for 30 min and incubated with 5 µg/ml diI-acLDL for 30 min at 4°C or 5 min at 37°C in the presence or absence of the drugs. Some cells were incubated with diI-acLDL in the presence of 250 µg/ml mBSA. Values of cell-associated fluorescence were calculated as total diI-acLDL minus the amount of diI-acLDL detected in the presence of mBSA, and are expressed as ng probe per mg protein. The amount of diI-acLDL detected in the presence of mBSA was always <400 ng probe per mg protein. Each value represents the mean ± SD of triplicate determinations in a typical experiment. Similar results were obtained in two separate experiments.
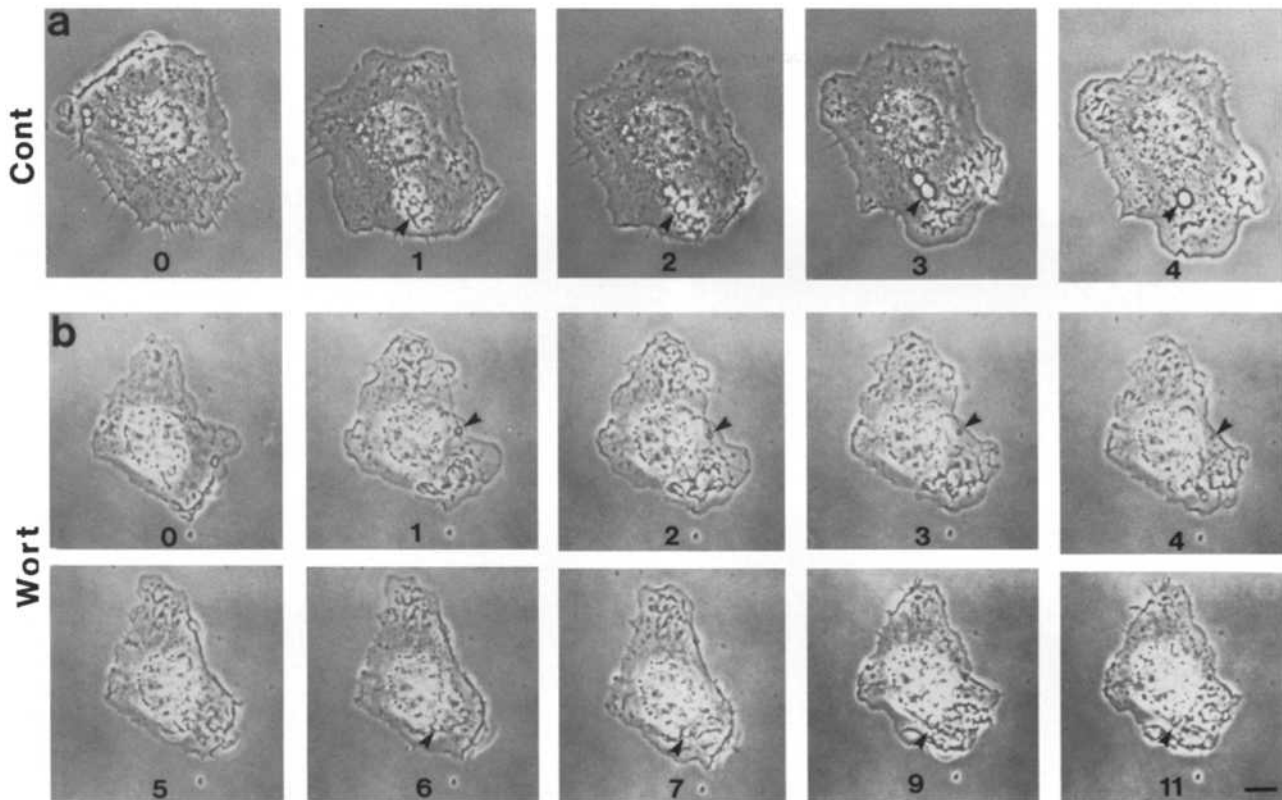
Figure 7. Time-lapse video microscopy of control and wortmannin-treated cells before and after addition of M-CSF. Macrophages on coverslips were treated with 0.1% DMSO (control; *a*) or 100 nM wortmannin for 30 min (*b*), and then observed by phase-contrast microscopy. Panels labeled 0 show macrophages before addition of M-CSF. Other panels indicate cells in 2,000 U/ml M-CSF. Numbers indicate time intervals (min) in the sequence. Ruffles are visible as phase-dense lines at the periphery of the cells. M-CSF increased ruffling in both control and wortmannin-treated cells. Circular ruffles closed into phase-bright macropinosomes in control cells (*arrowheads* in *a*), but receded into cytoplasm in wortmannin-treated cells (*arrowheads* in *b*). Bar, 10 μm.

ciate with other proteins that do. Models for Fc receptor function include PI 3-kinase as part of the signal cascade leading to phagocytosis (15, 22). The data presented here indicate that PI 3-kinase functions in Fc receptor–mediated phagocytosis, but not in the signaling for pseudopod extension.

PI 3-kinase does appear to be part of the early signaling that leads to the respiratory burst. Wortmannin inhibits agonist-induced responses but not phorbol ester–induced responses in neutrophils (1, 2), indicating that PI 3-kinase functions upstream of protein kinase C in that signaling cascade. However, in macrophages, wortmannin inhibited both M-CSF– and PMA-stimulated pinocytosis to the same extent, indicating that PI 3-kinase functions downstream of protein kinase C.

Our observations of macropinocytosis and phagocytosis indicate that PI 3-kinase mediates a mechanism that closes macropinosomes and phagosomes into intracellular vesicles. After exposure to wortmannin or LY294002, circular ruffles formed and receded into cytoplasm without closing into macropinosomes, and pseudopodia extended around sheep erythrocytes without enclosing them. Confocal microscopy showed phagocytic cups cradling erythrocytes in wortmannin-treated macrophages (Fig. 10).

Other studies have reported inhibited phagocytosis of opsonized sheep erythrocytes by wortmannin (22). How-

ever, in one study, phagocytosis of opsonized erythrocytes by bone marrow–derived macrophages was only slightly inhibited (2). The different results might reflect a difference in the methods used for osmotic lysis of uningested erythrocytes. Our preliminary experiments indicated that mild osmotic lysis, 20 s of exposure to water instead of 30 s, left some partially engulfed erythrocytes intact. In the study by Baggiolini et al. (2), erythrocytes were lysed with 15-s exposure to dilute PBS (9). It is possible that because wortmannin allows phagocytosis to proceed part of the way toward completion, the macrophages can construct a cytoskeletal cup that affords the erythrocytes protection against mild osmotic shock.

In summary, this study indicates that PI 3-kinase contributes to a late step in macropinocytosis and phagocytosis, probably the closure of ruffles and pseudopodia to form intracellular vesicles. It will be important next to characterize the role of PI 3-kinase in this closure mechanism.
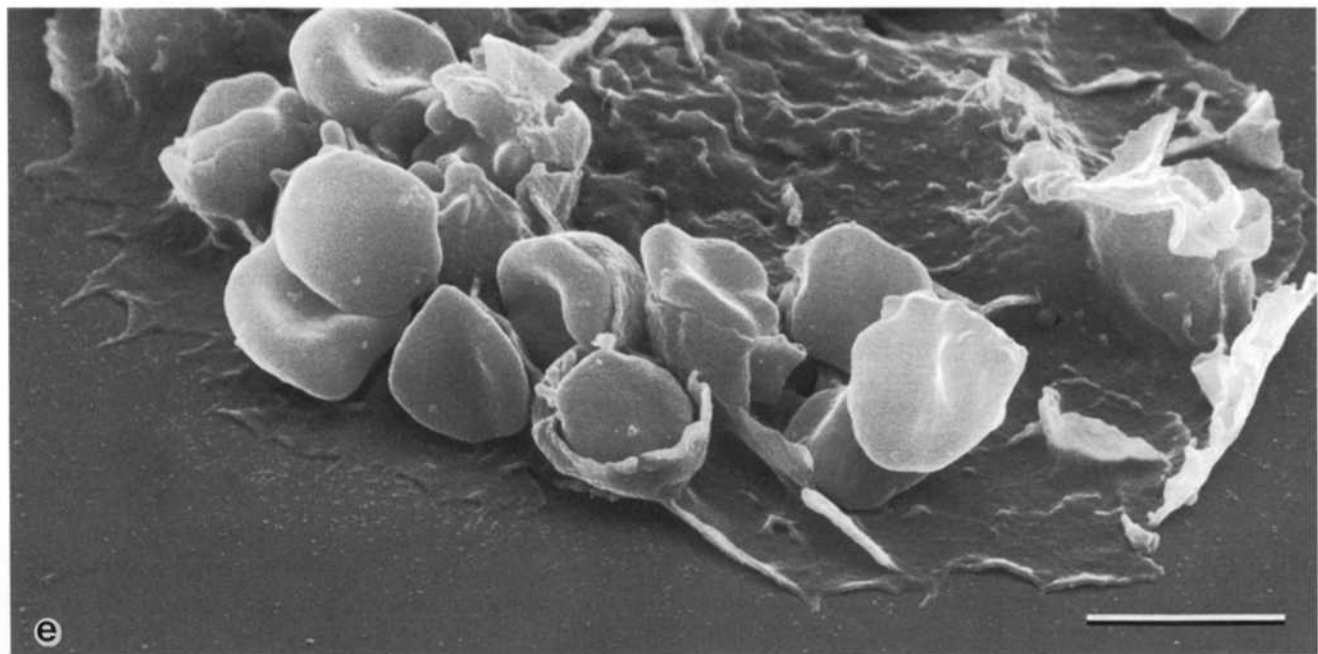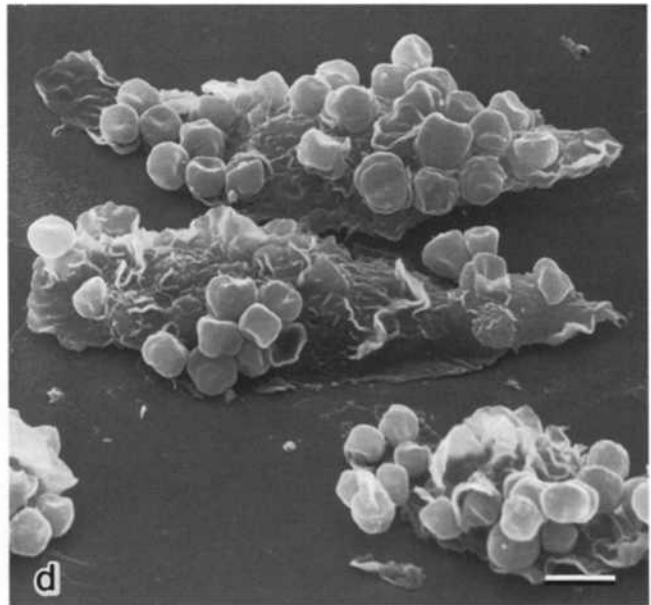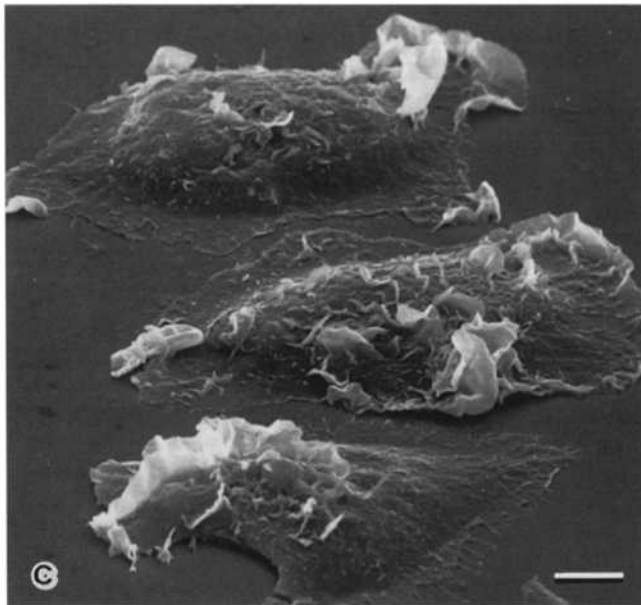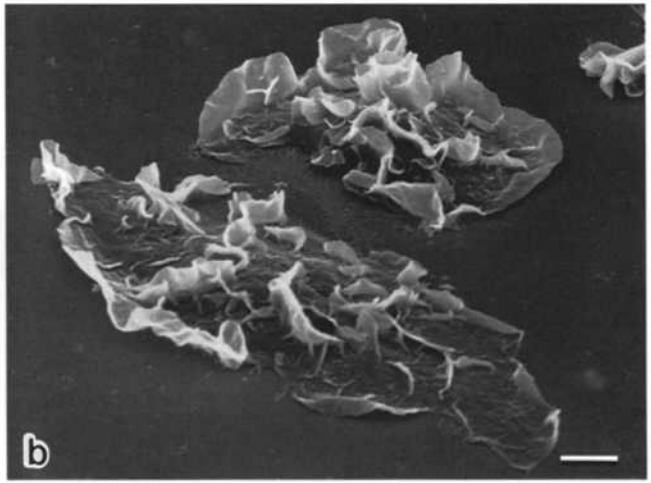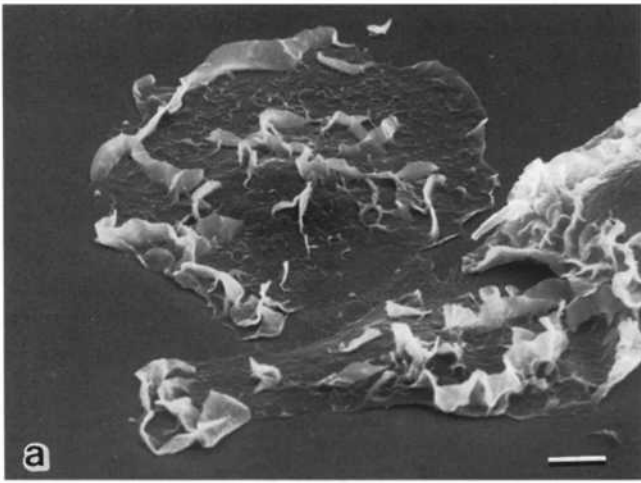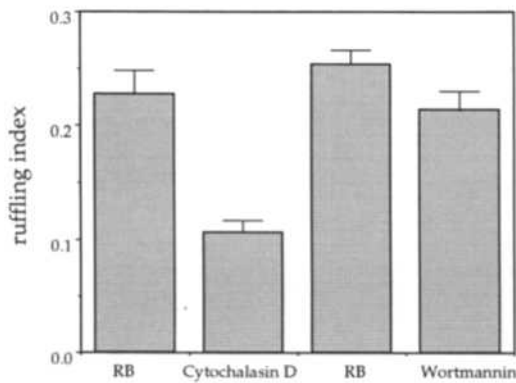
Figure 9. Quantitative measurements of ruffling in macrophages. Pairs of digitized, phase-contrast images of macrophages, separated by an interval of 15 s, were analyzed as described in Materials and Methods. The ruffling indices measure the fraction of pixels in the cell area of one image that differ by >20 gray units from the corresponding pixels in the second image. In control preparatons (*RB*), 21–26% of the pixels differed by that much. Treatment with cytochalasin D inhibited ruffling movements and lowered the index. Wortmannin inhibited ruffling slightly. The two RB plots are to the left of their corresponding experimental conditions. Bars show mean and standard error. Data are cumulative measurements from three or four separate experiments; $n = 15$ (cytochalasin D experiments) and 20 (wortmannin experiments).

Figure 10. Fluorescence confocal microscopy of macrophage phagocytosis. F-actin is labeled with rhodamine-phalloidin (*red*). IgG-opsonized erythrocytes are surface labeled with biotin and fluorescein-streptavidin (*green*). In this wortmannin-treated macrophage, pseudopodia extend halfway around the erythrocytes. Control preparations showed intracellular erythrocytes and no phagocytic cups (not shown). Bar, 10 μm.

References

1. Arcaro, A., and M.P. Wymann. 1993. Wortmannin is a potent phosphatidylinositol 3-kinase inhibitor: the role of phosphatidylinositol 3,4,5-trisphosphate in neutrophil responses. *Biochem. J.* 296:297–301.
2. Baggiolini, M., B. Dewald, J. Schnyder, W. Ruch, P.H. Cooper, and T.G. Payne. 1987. Inhibition of the phagocytosis-induced respiratory burst by the fungal metabolite wortmannin and some analogues. *Exp. Cell Res.* 169:408–418.
3. Barker, S.A., K.K. Caldwell, A. Hall, A.M. Martinez, J.R. Pfeiffer, J.M. Oliver, and B.S. Wilson. 1995. Wortmannin blocks lipid and protein kinase activities associated with PI 3-kinase and inhibits a subset of responses induced by FcεR1 cross-linking. *Mol. Biol. Cell.* 6:1145–1158.
4. Berthiaume, E.P., C. Medina, and J.A. Swanson. 1995. Molecular size-fractionation during endocytosis in macrophages. *J. Cell Biol.* 129:989–998.
5. Brown, W.J., D.B. DeWald, S.D. Emr, H. Plutner, and W.E. Balch. 1995. Role for phosphatidylinositol 3-kinase in the sorting and transport of newly synthesized lysosomal enzymes in mammalian cells. *J. Cell Biol.* 130:781–796.
6. Cantley, L.C., K.R. Auger, C. Carpenter, B. Duckworth, A. Graziani, R. Kapeller, and S. Soltoff. 1991. Oncogenes and signal transduction. *Cell.* 64:281–302.
7. Carlberg, K., P. Tapley, C. Haystead, and L. Rohrschneider. 1991. The role of kinase activity and the kinase insert region in ligand-induced internalization and degradation of the c-fms protein. *EMBO (Eur. Mol. Biol. Organ.) J.* 10:877–883.
8. Clague, M.J., C. Thorpe, and A.T. Jones. 1995. Phosphatidylinositol 3-kinase regulation of fluid phase endocytosis. *FEBS Lett.* 367:272–274.
9. Cooper, P.H., P. Mayer, and M. Baggiolini. 1984. Stimulation of phagocytosis in bone marrow-derived mouse macrophages by bacterial lipopolysaccharide: correlation with biochemical and functional parameters. *J. Immunol.* 133:913–922.
10. Davidson, H.W. 1995. Wortmannin causes mistargeting of procathepsin D. Evidence for the involvement of a phosphatidylinositol 3-kinase in vesicular transport to lysosomes. *J. Cell Biol.* 130:797–805.
11. de Camilli, P., S.D. Emr, P.S. McPherson, and P. Novick. 1996. Phosphoinositides as regulators of membrane traffic. *Science (Wash. DC).* 271: 1533–1539.
12. Fukuda, S., S. Horiuchi, K. Tomita, M. Murakami, Y. Morino, and K. Takahashi. 1986. Acetylated low-density lipoprotein is endocytosed through coated pits by rat peritoneal macrophages. *Virchows Arch.* 52:1–13.
13. Goldstein, J.L., Y.K. Ho, S.K. Basu, and M.S. Brown. 1979. Binding site on macrophages that mediates uptake and degradation of acetylated low density lipoprotein, producing massive cholesterol deposition. *Proc. Natl. Acad. Sci. USA.* 76:333–337.
14. Gout, I., R. Dhand, I.D. Hiles, M.J. Fry, G. Panayotou, P. Das, O. Truong, N.F. Totty, J. Hsuan, G.W. Booker, I.D. Campbell, and M.D. Waterfield. 1993. The GTPase dynamin binds to and is activated by a subset of SH3 domains. *Cell.* 75:25–36.
15. Greenberg, S. 1995. Signal transduction of phagocytosis. *Trends Cell Biol.* 5:93–99.
16. Joly, M., A. Kazlauskas, and S. Corvera. 1995. Phosphatidylinositol 3-kinase activity is required at a post-endocytic step in platelet-derived growth factor receptor trafficking. *J. Biol. Chem.* 270:13225–13230.
17. Kodama, T., M. Freeman, L. Rohrer, J. Zabrecky, P. Matsudaira, and M. Krieger. 1990. Type I macrophage scavenger receptor contains α-helical and collagen-like coiled-coils. *Nature (Lond.).* 343:531–535.
18. Kotani, K., K. Yonezawa, K. Hara, H. Ueda, Y. Kitamura, H. Sakaue, A. Ando, A. Chavanieu, B. Calas, F. Grigorescu, M. Nishiyama, M.D. Waterfield, and M. Kasuga. 1994. Involvement of phosphoinositide 3-kinase in insulin- or IGF-1-induced membrane ruffling. *EMBO (Eur. Mol. Biol. Organ.) J.* 13:2313–2321.
19. Li, G., C. D'Souza-Schorey, M.A. Barbieri, R.L. Roberts, A. Klippel, L.T. Williams, and P.D. Stahl. 1995. Evidence for phosphatidylinositol 3-kinase as a regulator of endocytosis via activation of Rab5. *Proc. Natl. Acad. Sci. USA.* 92:10207–10211.
20. Liscovitch, M., and L.C. Cantley. 1995. Signal transduction and membrane traffic: the PITP/phosphoinositide connection. *Cell.* 81:659–662.

Figure 8. Scanning electron micrographs of ruffling and incomplete phagocytosis in wortmannin-treated macrophages. (*a*) Control macrophages. (*b*) Macrophages treated with 100 nM wortmannin for 30 min. (*c*) Control macrophages after 30 min phagocytosis of opsonized sheep erythrocytes; cells have completed phagocytosis. (*d* and *e*) Wortmannin-treated macrophages fed opsonized sheep erythrocytes for 30 min. (*e*) Higher magnification of phagocytic cups in wortmannin-treated cells. Bars, 5 μm.

21. Nakanishi, S., K.J. Catt, and T. Balla. 1995. A wortmannin-sensitive phosphatidylinositol 4-kinase that regulates hormone-sensitive pools of inositol phospholipids. *Proc. Natl. Acad. Sci. USA.* 92:5317–5321.

22. Ninomiya, N., K. Hazeki, Y. Fukui, T. Seya, T. Okada, O. Hazeki, and M. Ui. 1994. Involvement of phosphatidylinositol 3-kinase in Fcγ receptor signaling. *J. Biol. Chem.* 269:22732–22737.

23. Racoosin, E.L., and J.A. Swanson. 1989. Macrophage colony-stimulating factor (rM-CSF) stimulates pinocytosis in bone marrow-derived macrophages. *J. Exp. Med.* 170:1635–1648.

24. Racoosin, E.L., and J.A. Swanson. 1992. M-CSF-induced macropinocytosis increases solute endocytosis but not receptor-mediated endocytosis in mouse macrophages. *J. Cell Sci.* 102:867–880.

25. Schu, P.V., K. Takegawa, M.J. Fry, J.H. Stack, M.D. Waterfield, and S.D. Emr. 1993. Phosphatidylinositol 3-kinase encoded by yeast VPS34 gene essential for protein sorting. *Science (Wash. DC).* 260:88–91.

26. Shepherd, P.R., M.A. Soos, and K. Siddle. 1995. Inhibitors of phosphoinositide 3-kinase block exocytosis but not endocytosis of transferrin receptors in 3T3-L1 adipocytes. *Biochem. Biophys. Res. Comm.* 211:535–539.

27. Shepherd, P.R., B.J. Reaves, and H.W. Davidson. 1996. Phosphoinositide 3-kinases and membrane traffic. *Trends Cell Biol.* 6:92–97.

28. Shpetner, H., M. Joly, D. Hartley, and S. Corvera. 1996. Potential sites of PI-3 kinase function in the endocytic pathway revealed by the PI-3 kinase inhibitor, wortmannin. *J. Cell Biol.* 132:595–605.

29. Spiro, D.J., W. Boll, T. Kirchhausen, and M. Wessling-Resnick. 1996. Wortmannin alters the transferrin receptor endocytic pathway in vivo and in vitro. *Mol. Biol. Cell.* 7:355–367.

30. Swanson, J.A. 1989. Phorbol esters stimulate macropinocytosis and solute flow through macrophages. *J. Cell Sci.* 94:135–142.

31. Swanson, J.A., and S.C. Baer. 1995. Phagocytosis by zippers and triggers. *Trends Cell Biol.* 5:89–93.

32. Swanson, J.A., and C. Watts. 1995. Macropinocytosis. *Trends Cell Biol.* 5: 424–428.

33. Thelen, M., M.P. Wymann, and H. Langen. 1994. Wortmannin binds specifically to 1-phosphatidylinositol 3-kinase while inhibiting guanine nucleotide-binding protein-coupled receptor signaling in neutrophil leukocytes. *Proc. Natl. Acad. Sci. USA.* 91:4960–4964.

34. van der Bliek, A.M., T.E. Redelmeier, H. Damke, E.J. Tisdale, E.M. Meyerowitz, and S.L. Schmid. 1993. Mutations in human dynamin block an intermediate stage in coated vesicle formation. *J. Cell Biol.* 122:553–563.

35. Vlahos, C.J., W.F. Matter, K.Y. Hui, and R.F. Brown. 1994. A specific inhibitor of phosphatidylinositol 3-kinase, 2-(4-morpholinyl)-8-phenyl-4H-1-benzopyran-4-one (LY294002). *J. Biol. Chem.* 269:5241–5248.

36. Wennström, S., P. Howkins, F. Cooke, K. Hara, K. Yonezawa, M. Kasuga, T. Jackson, L. Claesson-Welsh, and L. Stephens. 1994. Activation of phosphoinositide 3-kinase is required for PDGF-stimulated membrane ruffling. *Curr. Biol.* 4:385–393.

37. Wright, S.D., and S.C. Silverstein. 1982. Tumor-promoting phorbol esters stimulate C3b and C3b' receptor-mediated phagocytosis in cultured human monocytes. *J. Exp. Med.* 156:1149–1164.

38. Yano, H., S. Nakanishi, K. Kimura, N. Hanai, Y. Saitoh, Y. Fukui, Y. Nonomura, and Y. Matsuda. 1993. Inhibition of histamine secretion by wortmannin through the blockade of phosphatidylinositol 3-kinase in RBL-2H3 cells. *J. Biol. Chem.* 268:25846–25856.

39. Yano, H., T. Agatsuma, S. Nakanishi, Y. Saitoh, Y. Fukui, Y. Nonomura, and Y. Matsuda. 1995. Biochemical and pharmacological studies with KT7692 and LY294002 on the role of phosphatidylinositol 3-kinase in FcεRI-mediated signal transduction. *Biochem. J.* 312:145–150.